

Two Ring Nebulae around Blue Supergiants in the Large Magellanic Cloud

K. Weis^{1,2*}, Y.-H. Chu^{2*}, W.J. Duschl^{1,3}, and D.J. Bomans^{2*,**}

¹ Institut für Theoretische Astrophysik, Tiergartenstr. 15, D-69121 Heidelberg, Germany

² University of Illinois, Department of Astronomy, 1002 W. Green Street, Urbana, IL 61801, USA

³ Max-Planck-Institut für Radioastronomie, Auf dem Hügel 69, D-53121 Bonn, Germany

received; accepted

Abstract. Ring nebulae are often found around massive stars such as Wolf-Rayet stars, OB and Of stars and Luminous Blue Variables (LBVs). In this paper we report on two ring nebulae around blue supergiants in the Large Magellanic Cloud. The star Sk–69 279 is classified as O9f and is surrounded by a closed shell with a diameter of 4.5 pc. Our echelle observations show an expansion velocity of 14 km s^{-1} and a high $[\text{N II}]\lambda 6583\text{\AA}/\text{H}\alpha$ ratio. This line ratio suggests nitrogen abundance enhancement consistent with those seen in ejectas from LBVs. Thus the ring nebula around Sk–69 279 is a circumstellar bubble.

The star Sk–69 271, a B2 supergiant, is surrounded by an $\text{H}\alpha$ arc resembling an half shell. Echelle observations show a large expanding shell with the arc being part of the approaching surface. The expansion velocity is $\sim 24 \text{ km s}^{-1}$ and the $[\text{N II}]\lambda 6583\text{\AA}/\text{H}\alpha$ is not much higher than that of the background emission. The lack of nitrogen abundance anomaly suggests that the expanding shell is an interstellar bubble with a dynamic age of $2 \times 10^5 \text{ yr}$.

Key words: Stars: circumstellar matter – Stars: evolution – Stars: individual: Sk–69 271 – Stars: individual: Sk–69 279 – Stars: mass-loss – ISM: bubbles

1. Introduction

Massive stars are known to have strong stellar winds and lose a lot of mass. For example, stars with an initial mass

Send offprint requests to: K. Weis,
email: kweis@ita.uni-heidelberg.de

* Visiting Astronomer, Cerro Tololo Inter-American Observatory, National Optical Astronomy Observatories, operated by the Association of Universities for Research in Astronomy, Inc., under contract with the National Science Foundation.

** Feodor-Lynen Fellow of the Alexander von Humboldt Foundation

above $35 M_{\odot}$ will lose 50% or more of their mass before their demise (García-Segura et al. 1996a, 1996b). These stars have a large impact on the interstellar environments and influence the circumstellar surroundings throughout their evolutionary phases. Ring nebulae around massive stars testify the effects of stellar mass loss, as they are formed by fast stellar wind sweeping up ambient interstellar medium, fast wind interacting with previous slow wind, or outburst-like ejection of stellar material (Castor et al. 1975; Weaver et al. 1977; Chu 1991).

All massive stars that experience fast stellar winds either currently or previously, e.g. OB supergiants, ought to be surrounded by ring nebulae. Surprisingly, only a handful of ring nebulae around O supergiants, but not B supergiants, are known in our galaxy (Lozinskaya 1982; Chu 1991); no ring nebulae around single O or B supergiants are known in the Large Magellanic Cloud (LMC), which otherwise hosts a large collection of shell nebulae of all sizes (e.g. Davies et al. 1976). While the scarcity of known ring nebulae around OB supergiants could be caused by the lack of a sensitive systematic survey, other causes cannot be excluded.

Recently, we found two ring nebulae around blue supergiants in the LMC: a closed shell with a $18''$ diameter around the star Sk–69 279 (designation from Sanduleak 1969), and a half shell of $21''$ diameter around the star Sk–69 271 (Weis et al. 1995). As shown in Fig. 1, both stars are located to the north-east of the H II region N 160 (designation from Henize 1956). We have obtained additional images of this field and high-dispersion long-slit echelle spectra of these ring nebulae in $\text{H}\alpha$ and $[\text{N II}]$ lines. These data allow us to determine not only the physical structure of the nebulae, but also diagnostics for N abundance in the nebulae, which can be used to constrain the evolutionary states of the central stars.

This paper reports our analysis of the ring nebulae around Sk–69 271 and Sk–69 279. Section 2 describes the observations and reductions of the data; sections 3 and 4

describe our findings for Sk-69 279 and Sk-69 271, respectively. We discuss the formation and evolution of these two ring nebulae in section 5, and conclude in section 6.

2. Observation and data reduction

2.1. Imaging

We obtained CCD images with the 0.9 m telescope at Cerro Tololo Inter-American Observatory (CTIO) in January 1996. The 2048×2048 Tek2K3 CCD used had a pixel size of $0''.4$. The field of view was $13'.5 \times 13'.5$, large enough to encompass both Sk-69 279 and Sk-69 271. Broadband Johnson-Cousins B, V, R filters and narrow-band $H\alpha$ and [OIII] filters were used. The $H\alpha$ filter had a central wavelength of 6563 \AA and a filter width of 75 \AA , which included the [NII] lines at 6548 \AA and 6583 \AA . The [OIII] filter had a central wavelength of 5007 \AA and a width of 44 \AA . The exposure time was between 10 and 300 s for the B, V and R filters and 900 s for $H\alpha$ and [OIII]. The seeing was around $2''$ during the observations; the sky condition was not photometric.

Fig. 1 displays a $6' \times 3'.5$ sub-field of the $H\alpha$ image to show the ring nebulae around Sk-69 279 and Sk-69 271 and their relationship to the H II region N160. We have subtracted a scaled R frame from the $H\alpha$ image to obtain a continuum-free $H\alpha$ frame. Several stars in the field were used for the scaling. The continuum-subtracted $H\alpha$ images ($1' \times 1'$) of the two ring nebulae are shown in Fig. 2a and 2b. Not all continuum sources were removed well and some white parts in the images mark the residuals. Neither of the ring nebula showed emission in the [O III] filter.

We performed a flux calibration of our $H\alpha$ image using a photo-electrically calibrated PDS scan of Kennicutt & Hodge's (1986) Curtis Schmidt plate, kindly provided to us by Dr. R.C. Kennicutt. We transferred the calibration by using the fluxes of two compact emission knots and three narrow $H\alpha$ filaments near N160 that were visible in both our CCD images and their Schmidt plate. The different spatial resolutions and the variable background levels made the largest contributions to the uncertainty in the calibration. We estimate that the error in the flux calibration should be much less than 30%.

2.2. Echelle spectroscopy

To investigate the kinematic structure of the two ring nebulae, we obtained high-dispersion spectroscopic observations with the echelle spectrograph on the 4 m telescope at CTIO in January 1996. We used the long-slit mode, inserting a post-slit $H\alpha$ filter ($6563/75 \text{ \AA}$) and replacing the cross-disperser with a flat mirror. A 791 mm^{-1} echelle grating was used. The data were recorded with the long focus red camera and the 2048×2048 Tek2K4 CCD. The pixel size was $0.08 \text{ \AA pixel}^{-1}$ along the dispersion and $0'.26 \text{ pixel}^{-1}$ in the spatial axis. The slit length was effectively limited by vignetting to $\sim 4'$. Both $H\alpha$ 6563 \AA

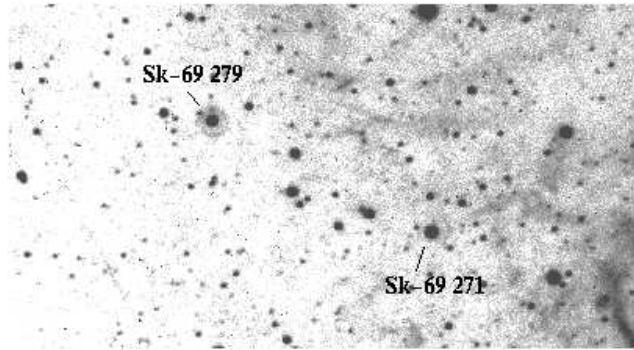


Fig. 1. $H\alpha$ image of the region including both ring nebulae. North is up, and east is to the left. The field of view is $6' \times 3'.5$. The bright $H\alpha$ emission to the west belongs to the H II region N160. Sk-69 279 is surrounded by a closed shell, and Sk-69 271 a half-shell. The straight line near the eastern edge is caused by a satellite crossing the field of view.

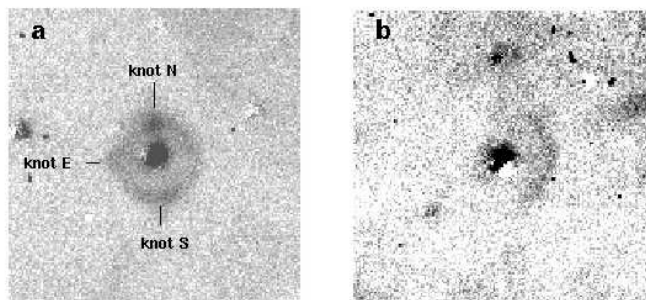


Fig. 2. Continuum-subtracted $H\alpha$ images of the ring nebulae around: (a) Sk-69 279, (b) Sk-69 271. North is up, and east is to the left. Each image covers $1' \times 1'$.

and [NII] 6548 \AA , 6583 \AA lines were covered in the setup. The slit-width was $250 \mu\text{m}$ ($\cong 1''.64$) and the instrumental FWHM was about 14 km s^{-1} at the $H\alpha$ line. The seeing was $\sim 2''$ during the observations. Thorium-Argon comparison lamp frames were taken for wavelength calibration and geometric distortion correction. The reduction of all images and spectra was done in IRAF.

For the ring around Sk-69 279 two east-west oriented slit positions were observed, one centered on the star itself and the other with a $4''$ offset to the north. The ring around Sk-69 271 was observed with only one east-west oriented slit centered on the star.

The exposure time was 900 s for each position. Echelle images of the $H\alpha + [\text{N II}] \lambda 6583 \text{ \AA}$ lines are presented in Fig. 3. The spectral range shown here is from 6560 \AA to 6600 \AA ; the spatial axis is $1'$ long in Fig. 3a and 3b, and $2'$ long in Fig. 3c. Beside the $H\alpha$ and [NII] nebular lines, the geocoronal $H\alpha$ and three telluric OH lines (Osterbrock et al. 1996) can be seen (one telluric OH line is blended with the broad nebular $H\alpha$ line). These telluric lines provide conve-

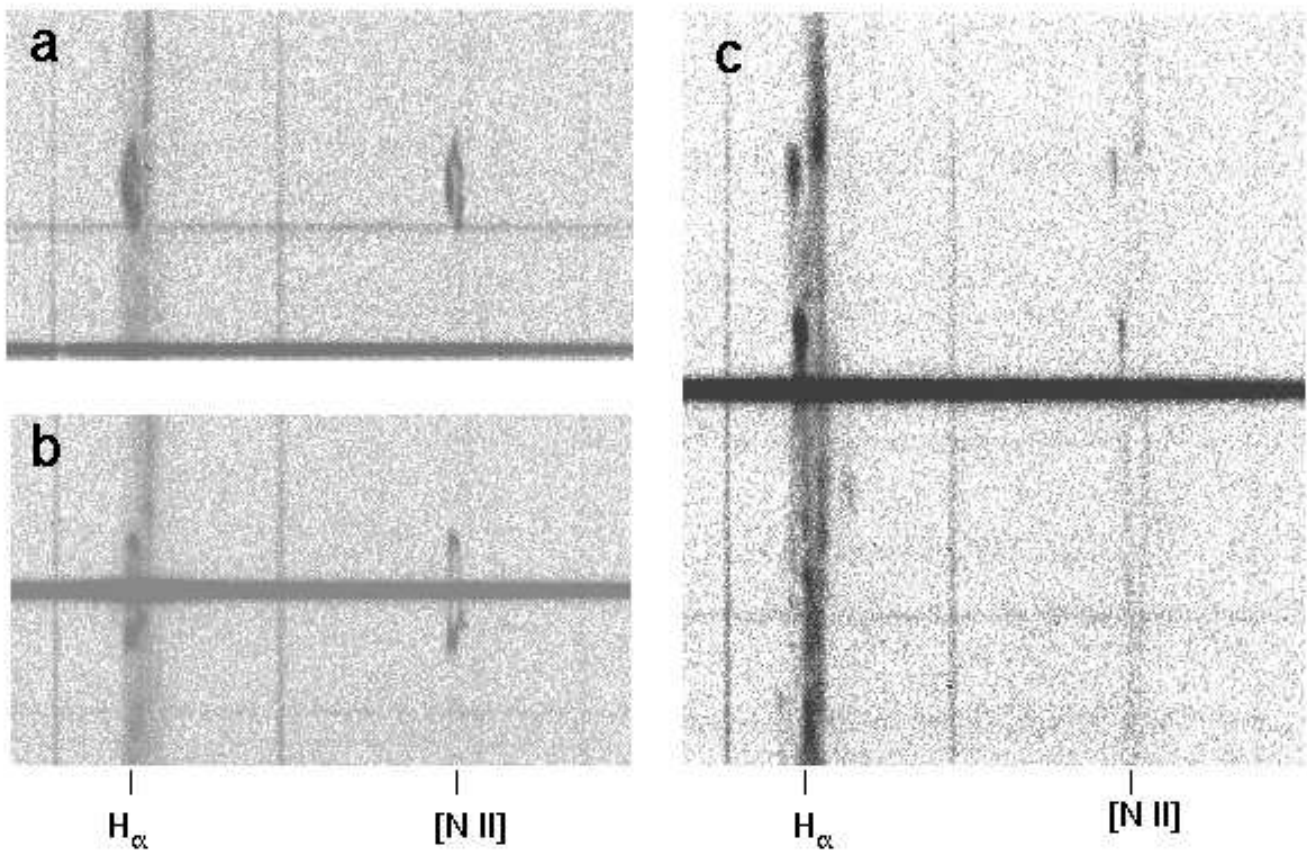


Fig. 3. Echellograms of the ring nebulae showing the $H\alpha$ line and the $[N II]\lambda 6583$ line: (a) centered at $4''$ north of Sk-69 279, (b) centered on the star Sk-69 279, (c) centered on Sk-69 271. The spectral axis (horizontal axis) covers from 6560 \AA to 6600 \AA , with wavelength increasing to the right. The spatial axis (vertical axis) is $1'$ long in panels a and b, and $2'$ long in panel c. West is up and east is down.

nient references for fine-tuning the wavelength calibration. All velocities given in this paper are heliocentric.

3. The ring nebula around Sk-69 279

Sk-69 279 is a blue supergiant, as its color and magnitude are $(B-V) = 0^m05$ and $V = 12^m79$ (Isserstedt 1975). Its spectral type was given by Rousseau et al. (1978) as O-B0, and was improved by Conti et al. (1986) to be O9f. With $T_{\text{eff}} = 30300 \text{ K}$ and $M_{\text{bol}} = -9^m72$ (Thompson et al. 1982), this star would be located in the very upper part of the HR diagram (Schaller et al. 1992), making it a massive star, maybe with an initial mass larger than $50 M_{\odot}$.

3.1. Structure and Morphology

As shown in Fig. 1 and 2a, the nebula around Sk-69 279 has a diameter of $18''$. Adopting a distance of 50 kpc to the LMC (Feast 1991), this angular size corresponds to a linear diameter of 4.5 pc. Fig. 1 shows that the nebula is most likely a closed spherical shell resembling a bub-

ble. Examined closely, the continuum-subtracted image (Fig. 2a) also reveals internal structure of the shell. There are surface brightness variations along the shell rim; furthermore, nebula emission extends beyond the shell rim in the north, south and east directions. We will call these extensions knot N, knot S and knot E, respectively. As described in section 3.2, some of these features show kinematic anomalies as well.

3.2. Kinematics of the nebula

For Sk-69 279 two long-slit echelle observations were made, one centered on the star and the other centered at $4''$ north of the star (Fig. 3a,b). Both the ring nebula and the background H II region are detected. The bow-shaped velocity structure originates from the ring nebula around Sk-69 279 and indicates an expanding shell. The broad $H\alpha$ component at a constant velocity corresponds to the background H II region at the outskirts of N160. Its central velocity at $v_{\text{hel}} \sim 250$ is similar to values found through Fabry-Perot measurements by

Caulet et al. 1982 (245.1 km s^{-1}) or Chériguene & Monnet 1972 (253.3 km s^{-1}). Also the main H I component in the vicinity of N 160 is of comparable size, at a velocity of 254 km s^{-1} (Rohlfs et al. 1984). The velocity profile of the background H II region with $\text{FWHM} \simeq 100 \text{ km s}^{-1}$, is much broader than those typically seen in classical H II regions, indicating a significant amount of turbulent motion.

To analyze the expansion pattern of the ring nebula we have made velocity-position plots, as shown in Fig. 4. The positions of the data points in the plots are distances from the star: the zero-point is the position of the central star, negative values are to the east and positive to the west. Measurements of both H α and [N II] lines are presented for Sk-69 279, but only H α for Sk-69 271. Their error bars are $\pm 4 \text{ km s}^{-1}$. The systemic velocity of the expanding shell, 230 km s^{-1} , is offset by 20 km s^{-1} with respect to the background H II region and the H I gas.

The position-velocity plot of the central slit position (Fig. 3b) shows typical characteristics of an expanding shell structure. In Fig. 3b the approaching side of the shell seems to reveal a constant velocity pattern instead of an expansion ellipse as seen in Fig. 3a. This may be explained by a very flat geometry of the shell at this position, e.g. nearly no curvature or result in an interaction of the shells approaching front with denser interstellar medium which halts the expansion. Despite the noticeable intensity variations in the shell, the expansion is relatively uniform. The expansion velocity is about 14 km s^{-1} in both H α and [N II] lines (see Fig. 4). However, a knot receding significantly faster than the general expansion is detected to the east of the central star (see Fig. 3b). This knot is indicated with a square in the position-velocity plot (lower plot in Fig. 4) and shows a velocity of about 272 km s^{-1} . This knot might be physically associated with the morphologically identified knot E.

Knot N was partially intercepted by the slit position at $4''$ north of the central star. It is most likely responsible for the intensity enhancement on the approaching side of the shell (Fig. 3a). In contrast to knot E, the velocity of knot N does not show noticeable deviation from the shell expansion.

Note that the line images of the central slit position (Fig. 3b) show larger intensity enhancement at the shell rims than those of the slit at $4''$ north (Fig. 3a). This difference in limb brightening is caused by the longer path length through the shell at central slit position.

In summary, the ring nebula around Sk-69 279 is a closed and uniform expanding shell. The morphologically identified knots show different kinematic characteristics. Knot N follows the shell expansion, while knot E shows large velocity anomaly.

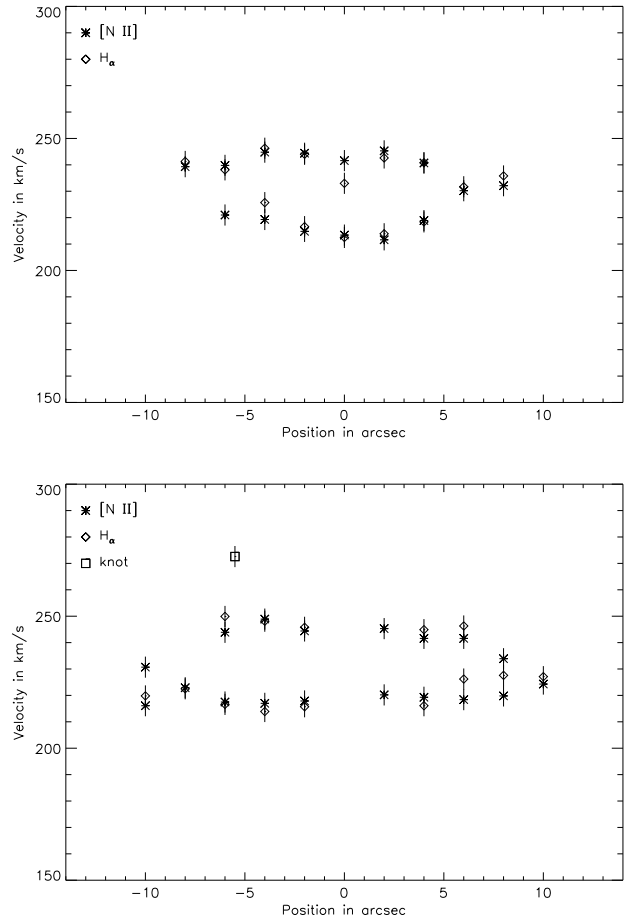


Fig. 4. Velocity-position plots for the nebula around Sk-69 279. The upper plot is derived from the echelle slit at $4''$ north of the star, and the zero point in the position axis is $4''$ due north of the star. The lower plot is derived from the slit centered on the star, and the zero point in the position axis is at the star. Negative offsets are to the east and positive to the west. Both H α and [N II] line measurements are plotted.

4. The nebula around Sk-69 271

The color and magnitude of Sk-69 271, $(B-V) = 0^m00$ and $V = 12^m01$ (Isserstedt 1975) are consistent with those of a blue supergiant in the LMC. Using objective prism spectra Rousseau et al. (1978) classified the star as B2. This spectral classification may be somewhat uncertain because of the low spectral resolution.

4.1. Structure and the morphology

Sk-69 271 is located in the outskirts of the H II region N 160 (Fig. 1). The nebula around Sk-69 271 consists of only one arc to the west side (Fig. 2b). It is not clear whether the eastern side is invisible because it is neutral or is missing because of a real lack of material. Assuming a complete round nebula, the diameter will be $21''$, or 5.3 pc .

Unlike the nebula around Sk–69 279, the nebula around Sk–69 271 is quite uniform and no clumps or knots are discernable.

4.2. Kinematics of the nebula

To determine the structure of the nebula around Sk–69 271 we obtained an east-west orientated long-slit echelle observation centered on the star. The line image (Fig. 3c) shows a complex velocity structure. An expanding shell structure centered on the star is present and extends over $70''$, or 17.7 pc. Both the approaching and receding side are detected with continuous distribution of material. The average line split near the shell center is about 48 km s^{-1} (Fig. 5). On the edge of the shell the split line converges to the velocity of the background H II region at about 248 km s^{-1} , marked by the dashed line in Fig. 5. The velocity width of the background H II region is 116 km s^{-1} . Superimposed on the expanding shell and the background H II region are additional high-velocity components scattering between 115 and 395 km s^{-1} .

Interestingly, the H α arc around Sk–69 271 corresponds to a brighter section near the center of the approaching side of the expanding shell, instead of marking the edge of the expanding shell (Fig. 2b and 3c). This brighter part appears to lead the expansion on the approaching side.

The velocity structure in the [N II] line is similar to that in the H α line. Unfortunately the [N II] line is too weak for accurate velocity measurements.

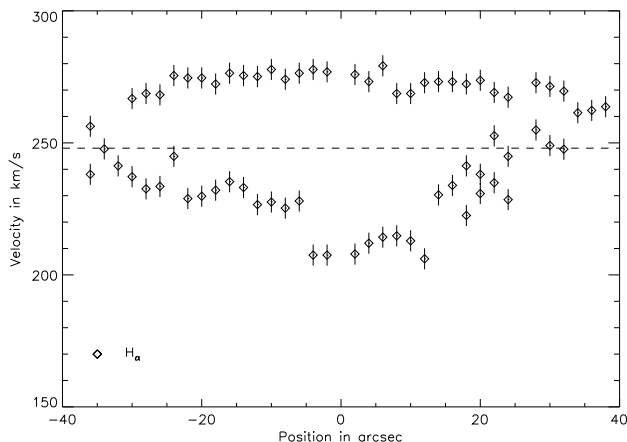


Fig. 5. Velocity-position plots for the nebula around Sk–69 271. Only H α measurements are plotted. The zero point in the position axis is centered on the star. Negative offsets are to the east and positive to the west. The dashed line marks the velocity of the background H II region. Only H α measurements are plotted; the [N II] lines are too weak for accurate measurements.

5. Discussion

5.1. The formation of ring nebulae

To determine the nature of the two ring nebulae around Sk–69 279 and Sk–69 271, it is worth looking into the mass loss history and how these winds interact with their environment to form ring nebulae.

In the main-sequence phase a fast stellar wind will sweep up the ambient medium to form a shell around the central star. These shells are called *interstellar bubbles* (Weaver et al. 1977) because they consist of mainly interstellar medium. An interstellar bubble blown by a $35 M_{\odot}$ in a medium of density 20 cm^{-3} can reach a typical radius of 38 pc at the end of the main-sequence phase (García-Segura et al. 1996b).

The most massive stars, with an initial mass $M_{ZAMS} \geq 50 M_{\odot}$, will lose half of their mass during the main-sequence stage before evolving into Luminous Blue Variables (LBVs). LBVs populate an area in the upper HR Diagram, called the Humphreys-Davidson limit (e.g. Humphreys & Davidson 1979; Humphreys & Davidson 1994; Langer et al. 1994). At this point of their evolution the stars are very unstable and have a very high mass loss rate around $10^{-4} M_{\odot} \text{ yr}^{-1}$. The strong stellar wind as well as the giant eruptions during this phase will strip a high amount of mass from the star, preventing the star from reaching the red supergiant phase. Since large amounts of mass have been ejected, LBVs are often surrounded by small circumstellar nebulae (Nota et al. 1995; García-Segura et al. 1996a).

Less massive stars never reach this unstable phase; instead they evolve into red supergiants after spending roughly 10^6 yr as main sequence O stars. A $35 M_{\odot}$ star will lose about $2.5 M_{\odot}$ during its main-sequence phase with a wind velocity of about 1000 km s^{-1} . At the red supergiant phase, the wind becomes slower ($\simeq 20 \text{ km s}^{-1}$) but much denser and a total amount of $18.6 M_{\odot}$ will be shed in the short ($2.3 \times 10^5 \text{ yr}$) time before the star turns into a Wolf-Rayet star or blue supergiant (García-Segura et al. 1996b).

The wind of an evolved star will contain processed material. The dense wind at the red supergiant phase or the LBV phase is enriched with CNO processed material. Consequently, a *circumstellar bubble*, formed by fast wind sweeping up the slow wind or a LBV nebula will show abundance anomaly.

These possible evolutionary scenarios predict the formation of different types of ring nebulae around massive stars. Furthermore, the physical properties of the ring nebulae are tied in with the evolutionary states of the central stars. By comparing the observational results of the ring nebulae of Sk–69 279 and Sk–69 271 with the predictions, we may determine the formation mechanism of the ring nebulae and the evolutionary state of these stars.

5.2. The nature of the nebula around Sk–69 279

The morphology of the ring nebula around Sk–69 279 suggests that it could be (1) an interstellar bubble blown by the star in the main sequence stage, (2) a circumstellar bubble formed by the blue supergiant wind sweeping up the previous red supergiant wind, or (3) a circumstellar bubble consisting of ejecta during an LBV phase of the star.

To distinguish among these possibilities we need to know the nitrogen abundance of the nebula. If the nitrogen abundance in the nebula is similar to that of the ambient interstellar medium, the bubble is most likely an interstellar bubble. If the nitrogen abundance is anomalous, it must contain processed stellar material. Since the LBV ejecta is more nitrogen enriched, as much as 13 times the original abundance (García-Segura et al. 1996a), than the RSG wind, which has 3 times the original abundance (García-Segura et al. 1996b), the degree of nitrogen enrichment in the nebulae can be used to differentiate between these two possibilities. To diagnose the nitrogen abundance we use the $[\text{NII}]\lambda 6583\text{\AA}/\text{H}\alpha$ ratio extracted from the echelle data.

The $[\text{NII}]\lambda 6583\text{\AA}/\text{H}\alpha$ ratio of the bubble is $\simeq 0.70 \pm 0.02$, while that of the background is only $\simeq 0.07 \pm 0.02$. Assuming similar ionisation and excitation conditions in the bubble and the ambient medium, a factor of 10 difference in the $[\text{NII}]\lambda 6583\text{\AA}/\text{H}\alpha$ ratio implies a factor of 10 enhancement in nitrogen abundance. Therefore it is likely that the bubble is nitrogen enhanced and contains stellar material. This enhancement is too high for a red supergiant wind, therefore this bubble probably contains LBV ejecta.

For a LBV nebula (LBVN), the expansion velocity of Sk–69 279’s ring, 14 km s^{-1} , is on the low end of the range reported for other LBVNs (Nota et al. 1995). However, the size of Sk–69 279’s ring, 4.5 pc , is larger than the other known LBVNs. The dynamic time, defined as (radius)/(expansion velocity), of Sk–69 279’s ring is $1.5 \cdot 10^5 \text{ yr}$, the largest among all known LBVNs. It is possible that the expansion has slowed down and the dynamic age of the nebula is really lower.

The origin of the curious feature knot E is not clear. It moves faster than the shell expansion, indicating that it belongs to a different kinematic system. Yet the $[\text{NII}]\lambda 6583\text{\AA}/\text{H}\alpha$ ratio of the knot is similar to those in the shell. It is possible that the knot originates from a later and faster ejection and appears to be interacting with the shell. It is also possible that the knot results from a fragmentation of the shell and has been accelerated by stellar wind. High resolution images and hydrodynamic modeling are needed to determine the nature of this knot.

5.3. The nature of the nebula around Sk–69 271

The morphology of the ring nebula around Sk–69 271, an arc, suggests a half-shell. Contrary to this impression the echelle spectra shows a large expanding shell (radius $\sim 9 \text{ pc}$) and the arc (radius $\sim 3 \text{ pc}$) is only a small part on the approaching side of the shell. To distinguish between the circumstellar and interstellar origin of the bubble, again we use the $[\text{NII}]\lambda 6583\text{\AA}/\text{H}\alpha$ ratio. We measured a ratio of 0.10 ± 0.02 in the expanding shell, 0.15 ± 0.02 in the arc, and 0.08 ± 0.02 in the ambient H II region. These values do not argue for a nitrogen abundance enhancement in the ring nebula, except possibly in the arc. Therefore, the shell consists mainly of interstellar material and is an interstellar bubble.

We have associated the arc with the shell, because it is very likely to be the result of an interaction of the bubble and an ambient interstellar filament or sheet. In such an interaction the projected shape of the interaction region will be dictated by the geometry of shell. This kind of interstellar features are probably common in this region at the outskirts of N 160, as the $\text{H}\alpha$ image (Fig. 1) shows filamentary structures in the vicinity and some of the filaments are detected at different velocities in the echelle data (Fig. 3c).

We can calculate the dynamic age of this interstellar bubble, $t_{\text{dyn}} = \eta(R/v_{\text{exp}})$, where R is the radius of the shell and v_{exp} the expansion velocity. $\eta = 0.6$ for an energy-conserving bubble (Weaver et al. 1977) or 0.5 for a momentum-conserving bubble (Steigman et al. 1975). The bubble around Sk–69 271 would have a kinematic age of about $2 \cdot 10^5 \text{ yr}$. Interestingly this age is smaller than the stars main-sequence life time. This may imply complexities in the stellar mass loss history and in the density structure of the interstellar environment.

Next we consider the ionisation of the nebula around Sk–69 271. The interstellar bubble is not clearly recognizable in the $\text{H}\alpha$ image, probably due to the combined effects of low surface brightness of the bubble and confusion from the many foreground/background filaments in this region. We integrated the $\text{H}\alpha$ flux within a radius of $35''$, the shell radius determined from the echelle data. The resulting $\text{H}\alpha$ flux, $9 \times 10^{34} \text{ erg s}^{-1}$, represents an upper limit for the shell, since it includes segments of possible foreground/background filaments. Converting the $\text{H}\alpha$ flux into the number of Lyman continuum photons necessary to ionize the gas, results in an upper limit of $\log N_{Ly\alpha} < 46.8$. We can compare this value with the model predictions (Panagia 1973), which give an ionizing flux of $\log N_{Ly\alpha} = 46.18$ for a B2 supergiant as Sk–67 271. Since we only could derive an upper limit for the necessary photon flux, it is still possible, that Sk–69 271 is responsible for the ionisation of the interstellar bubble.

6. Conclusion and summary

In this paper we report on two stars which have been found to be surrounded by ring nebulae. For Sk–69 279 we found a perfectly round ring structure and a high $[\text{N II}]\lambda 6583\text{\AA}/\text{H}\alpha$ ratio that indicates processed material. The ratio is 10 times higher than the background. Therefore we suggest this ring nebula to be an older LBV ejecta. No variability of the star or other signs of LBV activity have been reported, but the spectral type of Sk–69 279 is consistent with that of a quiescent LBV (Wolf 1992, Shore 1993).

For Sk–69 271 we found an arc in the $\text{H}\alpha$ image, but our echelle spectroscopic observation reveals a larger expanding shell with the arc being part of the approaching surface. The $[\text{N II}]\lambda 6583\text{\AA}/\text{H}\alpha$ ratio leads to the conclusion that the shell is an interstellar bubble.

Deep, high-resolution images are needed to study the fine-scale structure of the circumstellar bubble around Sk–69 279 and to reveal the morphology of the interstellar bubble around Sk–69 271. Variability observations of Sk–69 279 are needed to verify its LBV nature.

Acknowledgements. DJB thanks the Alexander von Humboldt Foundation for support through the Feodor Lynen Fellowship program.

References

- Castor J., Mc Cray R., Weaver R., 1975, ApJ 200, L107
 Caulet A., Deharveng L., Georgelin Y.M., Georgelin Y.P., 1982, A&A 110, 185
 Chériguene M.F., Monnet G., 1972, A&A 16, 28
 Chu Y.-H. 1991, in IAU Symp. 143, Wolf-Rayet Stars and Interrelations with Other Massive Stars in Galaxies, eds. K.A. van der Hucht and B. Hidayat, Kluwer, Dordrecht, Holland, p. 349
 Conti P.S., Garmany C.D., Massey P., 1986, AJ 92, 48
 Davies R.D., Elliott K.H., Meaburn J., 1976, MNRAS 81, 89
 Feast M.W., 1992, in Lectures Notes in Physics 416, New Aspects of Magellanic Cloud Research, eds. B. Baschek, G. Klare, J. Lequeux, Springer-Verlag, p. 239
 García-Segura G., Mac Low M.-M., Langer N., 1996a, A&A 305, 229
 García-Segura G., Langer N., Mac Low M.-M., 1996b, A&A 316, 133
 Henize K.G., 1956, ApJS 2, 315
 Humphreys R. M., Davidson K., 1979, ApJ 232, 409
 Humphreys R. M., Davidson K., 1994, PASP, 106, 1025
 Isserstedt J., 1975, A&AS 19, 259
 Kennicutt R.C., Hodge P.W., 1986, ApJ 306, 130
 Langer N., Hamann W.R., Lennon M. et al., 1994, A&A 290, 819
 Lozinskaya T.A., 1982, Ap&SS 87, 313
 Nota A., Livio M., Clampin M., Schulte-Ladbeck R., 1995, ApJ 448, 788
 Osterbrock D.E., Fulbright J.P., Martel A.R., Keane M.J., Trager S.C., Basri G., 1996, PASP 108, 277
 Panagia N., 1973, AJ 78, 929

- Rohlf K., Kreitschmann J., Siegman B.C., Feitzinger J.V., 1984, A&A 137, 343
 Rousseau J., Martin N., Prévot L., Rebeiro E., Robin A., Brunet J.P., 1977, A&AS 31, 243
 Sanduleak N., 1970, CTIO contribution 89
 Schaller G., Schaerer D., Meynet G., Maeder A., 1992, A&AS 96, 269
 Shore S.N., 1993, in ASP Conf. Ser. Vol. 35, Massive Stars: Their Lives in the Interstellar Medium, ed. J.P. Cassinelli and E.B. Churchwell, p. 186
 Steigman G., Strittmatter P.A., Williams R.E., 1975, ApJ 198, 575
 Thompson G.I., Nandy K., Morgan D.H., Willis A.J., Wilson R., Houziaux L., 1982, MNRAS 200, 551
 Weis K., Bomans D.J., Chu Y.-H., Joner M.D., Smith R.C., 1995, RevMexAASC, 3, 237
 Weaver R., McCray R.A., Castor J., Shapiro P., Moore R., 1977, ApJ 218, 377
 Wolf B., 1992, Reviews in Modern Astronomy 5, ed. G. Klare, Springer-Verlag, p. 1